

INVESTIGATION OF MECHANICAL AND STRUCTURAL ANISOTROPY OF N-A-XTRA 70  
MAG WELDMENTS

S. Sedmak,\* Lj. Nedeljković,\* A. Radović \*

The stress intensity factor  $K_Q$  determinations in 3-point bending and instrumented impact tests on trial MAG weldments of N-A-XTRA 70 steel 20 mm thick plates enabled that the deterioration in fracture toughness in HAZ be assessed in fracture mechanics terms.

INTRODUCTION

The fracture toughness determination across the weldment, from the base plate through the HAZ to the weld metal has been a subject of considerable practical and research (1-3) interest lately.

The objective of this investigation is to assess the effect of welding parameters on the fracture toughness in MAG weldments of quenched and tempered HSLA steel N-A-XTRA 70. In order to extend the toughness evaluation beyond the scope of usual Charpy V method, the stress intensity factor is determined on precracked specimens in 3-point bending tests, as well as the energy of crack initiation and crack propagation in the instrumented impact test.

To better elucidate the local structural and toughness changes in HAZ caused by a temperature cycling during welding in terms of base metal features, the base steel plate specimens are heat treated in the temperature range 500-1300°C after which the same mechanical properties as those in weldments are determined.

EXPERIMENTAL PART

Multipass 1/2 V/45° welds about 1 m long on 20 mm thick steel plates were made with different heat inputs and different speeds. The details of the weld specimen, as well as the mode the test pieces were cut from it, are given in Figure 1. The welds are made with Fluxofil 42 core wire of a 1,2 mm diameter, in pure CO<sub>2</sub> as shielding gas. The preheating and interpass temperature was 125°C. Welding parameters are listed in Table 1.

Chemical composition of the N-A-XTRA 70 steel plate, of the Fluxofil 42 wire, and of the weld metal in weld specimens are given in Table 2.

\* Faculty of Technology and Metallurgy, University of Belgrade, Yugoslavia

TABLE 1 - Welding Parameters for Technological Test Specimens

Specimen No.	Current J (A)	Voltage U (V)	Welding speed v (cm/min)	Heat input q (J/cm)	Number of Passes
2	140	22	25,22	5860	15
3	180	23	23,69	8390	8
4	220	24	22,96	11040	7
5	220	24	29,47	8600	8
6	135	21	16,40	8300	9

TABLE 2 - Composition of N-A-XTRA 70 Steel, Fluxofil 42 Wire and Weld Metals

Material		Composition, %										
		C	Si	Mn	Cr	Mo	Ni	P	S	Zr	Al	N
N-A-XTRA	70	0,16	0,61	0,94	0,77	0,34		0,012	0,012	0,07	0,014	0,0076
Fluxofil	42	0,05	0,35	1,50	0,50	0,40	2,4	-	-	-	-	-
Weld metal	2	0,08	0,37	1,02	0,48	0,33	1,78	-	-	-	-	-
Weld metal	3	0,07	0,30	1,20	0,62	0,40	2,06	-	-	-	-	-
Weld metal	4	0,09	0,36	1,21	0,61	0,37	1,71	-	-	-	-	-
Weld metal	5	0,09	0,25	1,12	0,45	0,40	1,82	-	-	-	-	-
Weld metal	6	0,08	0,21	1,10	0,40	0,38	1,86	-	-	-	-	-

TABLE 3 - Yield and Ultimate Tensile Strength of Welded Joints and Weld Metals

Heat Input q (J/cm)			5860	8390	11040	8600	8300
Yield point	$\sigma_Y$ (MPa)	Welded joint	700	740	746	733	722
		Weld metal	570	675	602	680	595
Ultimate Tensile Strength	UTS (MPa)	Welded joint	748	812	790	791	770
		Weld metal	630	722	665	722	644

RESULTS

The ultimate tensile and yield strength, the hardness across the weld, the stress intensity factor on 20x40x160 mm and 10x10x55 mm precracked test pieces at 20°C, and fracture energy in instrumented Charpy V test at -40°C are determined on all weld specimens made at different heat inputs. The same determinations are carried out on base plate specimens heat treated at different temperatures.

The yield and ultimate tensile strength values for welded joint and weld metal are given in Table 3. The hardness across the welds and weld macrographs are shown in Figure 2. The widths of HAZ in mm, also given in Figure 2, are average values obtained from measurements at three different levels on the vertical weld edge. The minimum widths are given in brackets. The tensile properties and hardness data for the base steel plate after holding it for 40 minutes at temperatures 500-1300°C in the furnace with subsequent cooling in air, are summarized in the diagram form in Figure 3.

The 3-point bending tests on precracked specimens are carried out in accordance with BS 5447. The  $K_Q$  values, obtained in those tests on heat treated base steel plates, are shown in diagram form in Figure 4, together with the  $K_Q$  values calculated for Charpy V notched specimens, tested at  $-40^{\circ}\text{C}$ , using maximum force from instrumented impact test diagram. The impact fracture energy, the energy of crack initiation and crack propagation for the base steel plate, heat treated in cited temperature range, are given in Table 4.

The results obtained in 3-point bending tests and Charpy V impact tests for test pieces cut from welded specimens are presented in Figure 5. The 1/2 V weld was chosen, in accordance with the recommendation of IIW, for easier determination of notch toughness in HAZ. The machined notch, and the resulting fatigue precrack tip was localized, as shown in Figure 1, at five different positions on vertical weld edge: in weld metal, on fusion line, in the base plate softened zone, and at 2 and 4 mm distance from fusion line.

TABLE 4 - Instrumented Impact Test Results for Heat Treated Base Plate Steel

Crack energy (J)	As delivered	Heat treatment temperature, $^{\circ}\text{C}$												
		500	600	650	700	750	800	900	1000	1050	1100	1150	1200	1300
Initiation	18	23	22	25	22	29	2,5	15	3	11	23	4	2	1,6
Propagation	19	20	17	21	19	29	2,5	15	3	8	19	3	0,8	2
Total	37	43	39	46	41	58	5,0	30	6	19	42	7	2,8	3,6

The microstructure of the base plate steel as delivered, i.e. after quenching in water and tempering at  $680^{\circ}\text{C}$ , consists of a mixture of ferrite and carbide. The transformation points of the steel are  $Ac_1 = 740^{\circ}\text{C}$  and  $Ac_3 = 870^{\circ}\text{C}$ . No microstructural changes could be detected microscopically in the samples heated 40 minutes at temperatures up to  $750^{\circ}\text{C}$  and subsequently cooled in air. Some coagulation of carbides, accompanied by better microscopic discerning of ferrite fields, takes place after normalizing at  $760^{\circ}\text{C}$ . In the samples normalized at temperatures  $800-900^{\circ}\text{C}$  the amount of bainite with some martensite rises at the cost of ferrite with rising temperature. Bands were made apparent in the microstructure, as shown in Fig.6, after normalizing in this temperature range, but above  $900^{\circ}\text{C}$  the banding disappears. The microstructure of samples normalized at  $900-1300^{\circ}\text{C}$  consists of upper bainite with some martensite.

#### DISCUSSION

The upper and lower dotted lines in each diagram in Figure 5, in which the fracture impact energies and  $K_Q$  values across the weld are plotted against heat input, represent the average values obtained for base plate steel heat treated at temperatures up to  $750^{\circ}\text{C}$  and above it, respectively. Although heat treated plate samples do not exactly simulate changes in HAZ, they can serve as limits of range in which the mechanical properties of HAZ could be expected to fall. Shifting of points towards the lower dotted line can be taken as a measure of the deterioration of the microstructure and fracture toughness in HAZ. The impact fracture energies across the weld, as shown in Figure 5a, b and c spread for all heat inputs round the upper base plate limit. The fact that not only some points, but also the average impact fracture energy for all points (Fig. 5a) exceeds the average base plate limit, can be accounted for by the fact, that the determinations were made at  $-40^{\circ}\text{C}$ , i.e. in the range of N-A-XTRA 70 transition temperature. The lowering of transition temperature in HAZ by several degree relative to N-A-XTRA 70 base plate was already observed in welds

made at lower inputs (1).

Contrary to the impact energy, the stress intensity factor values,  $K_Q$ , determined by instrumented impact and 3-point bending tests (Fig. 5d, e, f), do not, on the average, exceed the upper base plate limit. It means that  $K_Q$  is a more severe criterion for the deterioration within HAZ and the weld quality. The most significant in this respect is the fact that  $K_Q$  determined in the same instrumented impact test (Fig. 5d) falls entirely below the upper limit, while fracture energy (Fig. 5a) exceeds it.

The points of  $K_Q$  determined on the 10x10x55 mm precracked test pieces (Fig. 5e) are more shifted towards the lower base plate limit, thus becoming the most severe measure of deterioration in HAZ. The reason for this is not quite clear, but it might be assumed that, with decreasing specimen size, the local deterioration in HAZ can be better entailed.

$K_Q - \sigma_y$  ratio diagrams for instrumented impact (Fig. 7a) and three point bending tests (Fig. 7b) are the sound basis for consideration of weldment performance as a structural component. The ratio diagram is divided into four quadrants by straight lines drawn through the assumed  $K_{IC}$  and specified  $\sigma_y$  value for N-A-XTRA 70 grade steel.

Most of the points across the weld are gathered in quadrant 3, to which the points for unaffected base plate also pertain. By itself, it indicates a good quality of all welds, disregarding variations in heat input.

Points for base plate normalized at temperatures above 800°C are shifted into quadrant 1, obviously due to adverse microstructural changes.

The weld metal points in Figure 7, when plotted against yield point of weld metal instead of weldment, are situated in quadrant 2. It is a sign of undermatching, which by itself cannot be considered as detrimental to the weld performance (4). The effect of undermatching could be definitely assessed only by  $K_Q$  determination on weld metal after it had been work-hardened upon loading, but this requires further investigation.

The scatter of experimental points in Figures 5 and 7 makes it impossible for any distinctions to be made between the welds produced at various heat inputs, and this goes for the different parts within the same weldment. The cause of the scatter lies presumably not only in the local microstructural variations, but, to a great degree, also in the effect of banding. The type of banded structure found at some places in HAZ and caused by microsegregations of alloying elements, is shown in Figure 6c. The effect of banding, reflected in this case in the marked scatter of  $K_Q$  and impact energy values across the weld, was certainly less detrimental because of a favourable position of weld to the plate, so that longitudinal axis of test pieces coincided with the plate rolling direction. Otherwise, in the case of less favourable weld orientation the effect of banding should obviously be more stressed and more detrimental to the quality of weldment.

#### SUMMARY

The  $K_Q$  values of N-A-XTRA 70 weld specimens, as compared to those of unaffected base plate as well as to those of adversely affected base plate by normalizing, turned out to be more severe criterion of the deterioration in fracture toughness across the HAZ and weld metal than impact fracture energies.

REFERENCES

1. Degenkolbe, J., Uwer, D., 1974, *Schweissen & Schneiden* 26, No. 11-1.
2. Pellini, W. S., 1971, *Welding J.* 50, No. 3, Res. Suppl. 91-s.
3. Dawes, M. G., 1976, *Welding J.* 55, 1052.
4. Satoh, K., Toyoda, M., Ukita, K., Matsuura, T., 1979, *Welding J.* 58, No. 2, Res. Suppl. 25-s.

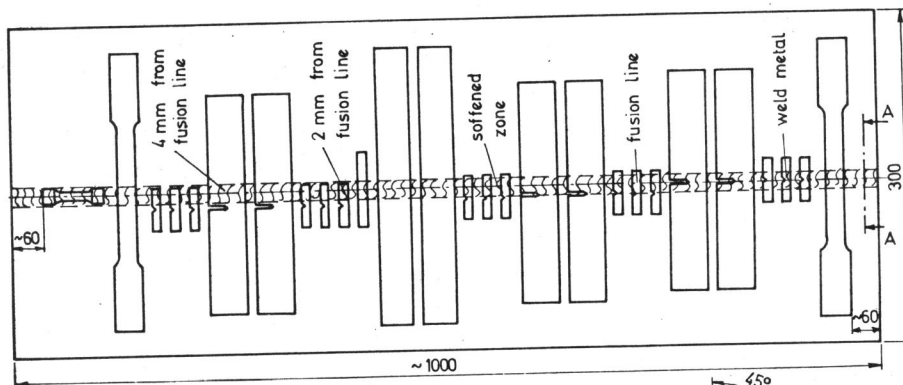


Figure 1 Welded specimen and disposition of test pieces

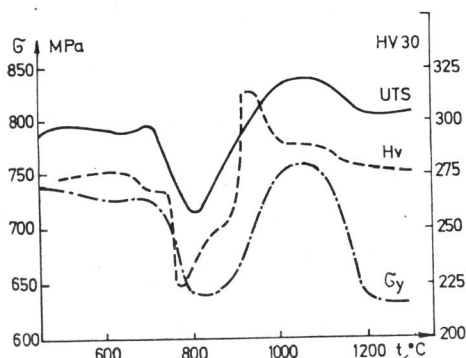


Figure 3 Yield and ultimate tensile strength of base metal against different temperatures of heat treatment

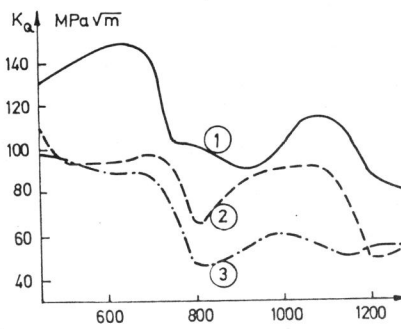


Figure 4 Stress intensity factors  $K_0$  against the temperature of heat treatment of base metal specimens for 10x10x55 precracked ① and 20x40x160 precracked ② test pieces, and for Charpy V ③ test pieces for maximum force in impact test

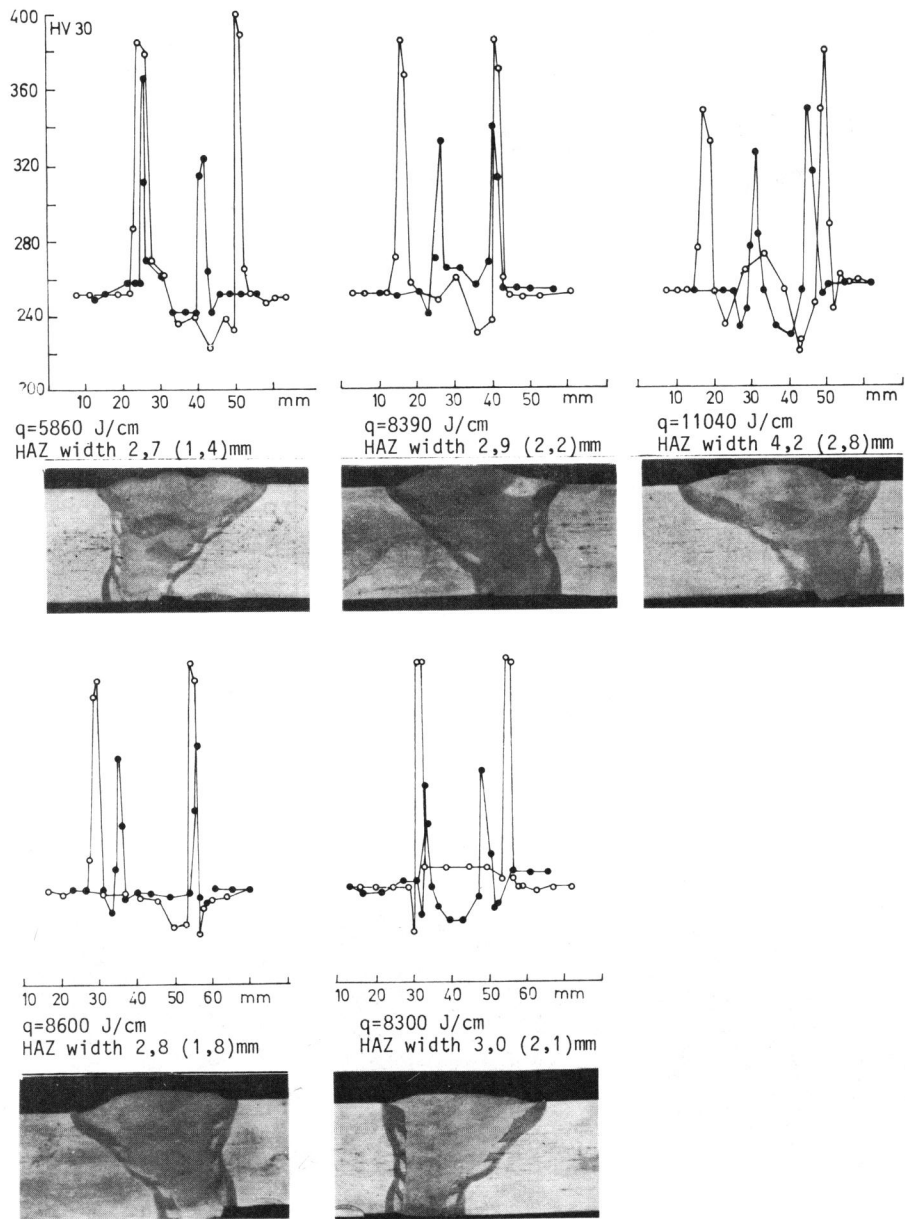


Figure 2 Macrographs and distribution of hardness in welded joints made at different heat inputs

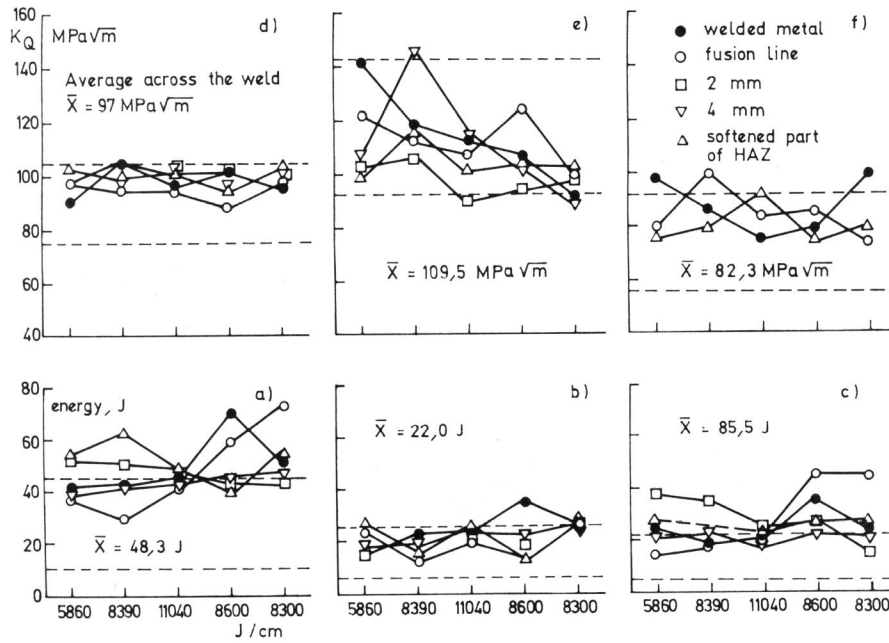


Figure 5 Total fracture energy (a), energy of crack initiation (b), and of crack propagation (c),  $K_Q$  determined in instrumented impact test (d), in 3-point bending test on 10x10x55 mm (e) and on 20x40x160 mm sample (f). The upper and lower dotted lines are corresponding mean values for the base plate specimens heat treated up to 750°C and above it, respectively

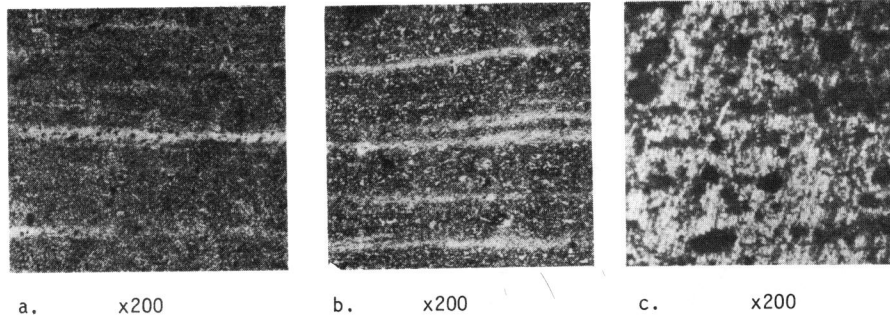


Figure 6 Banding in the base plate (a. and b.) and in HAZ (c.)

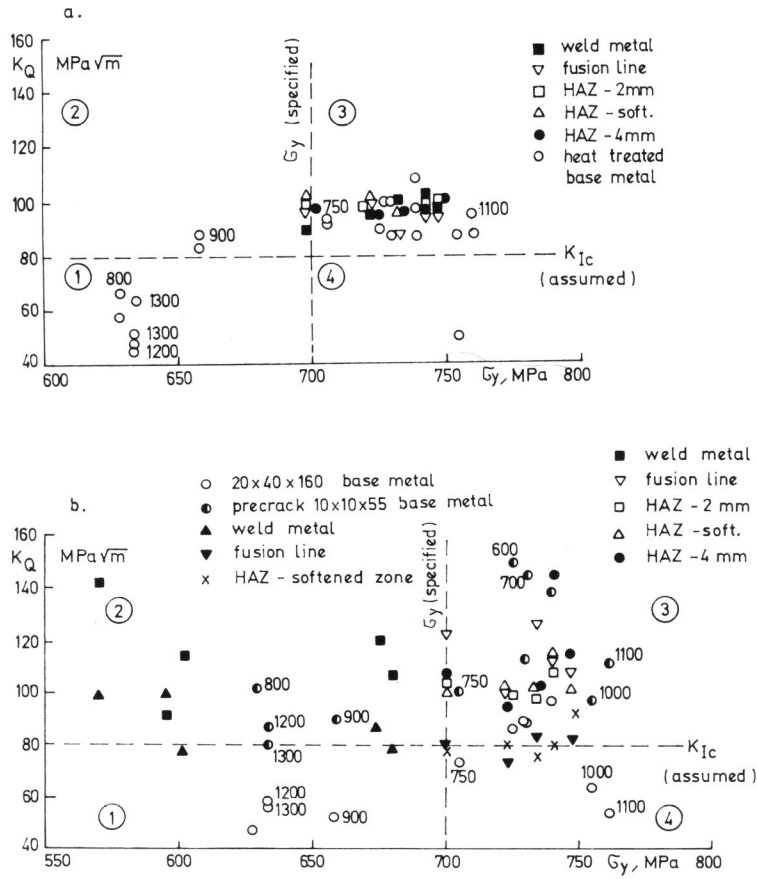


Figure 7 Stress intensity factor  $K_Q$ -yield stress  $\sigma_y$  correlations in instrumented impact tests (a) and three point bending tests (b) for welded joints and heat treated base metal